7-1-2005

Characterization Of Individual Submicron Perfluorocarbon Gas Bubbles By Ultrasonic Backscatter

E. Carr Everbach
Swarthmore College, ceverba1@swarthmore.edu

D. B. Khismatullin

J. T. Flaherty

R. A. Roy

Characterization of individual submicron perfluorocarbon gas bubbles by ultrasonic backscatter

E. Carr Everbach[a)]

Department of Engineering, Swarthmore College, 500 College Avenue, Swarthmore, PA 19081-1397
ceverba1@swarthmore.edu

Damir B. Khismatullin

Department of Biomedical Engineering, Duke University, Durham, NC 27708-0281
damir@duke.edu

John T. Flaherty

Transkaryotic Therapies Inc., 700 Main Street, Cambridge, MA 02139
jflaherty@tktx.com

Ronald A. Roy

Department of Aerospace and Mechanical Engineering, Boston University, 110 Cummington Street, Boston, MA 02215
ronroy@bu.edu

Abstract: Measurements were undertaken to determine the unknown microbubble-size distribution of a dodecafluoropentane (DDFP) emulsion consisting of 10^{12} droplets/ml in surfactant-stabilized water. The acoustic backscatter of 2-microsecond-duration tonebursts of 30-MHz focused ultrasound was measured from the emulsion as it moved in a coaxial flow. Calibration for the system was accomplished using 3-μm-radius polystyrene spheres, using a linear scattering model and literature values for polystyrene. Applying viscous linear scattering theory to the backscatter data from individual DDFP bubbles allowed inversion of the radius–backscatter relation. A mean microbubble radius of 130 nm was inferred for the DDFP population.
© 2005 Acoustical Society of America

1. Introduction

Determining the size distribution of preparations of microbubbles is an ongoing challenge in fields as diverse as oceanography[1] and biomedical ultrasound.[2] Various methods have been employed to interrogate large populations of microbubbles and yield ensemble-averaged parameters[3] that, in turn, provide information about bubble-size distributions. Methods that interrogate a single bubble at a time avoid these pitfalls,[4–6] although optical methods and Coulter counters have low sensitivity for bubbles smaller than about 1-μm radius.

Of great interest in biomedicine is the characterization of echocontrast agents used in biomedical ultrasound applications such as cardiology.[7] Of interest here are emulsions of dodecafluoropentane (DDFP) droplets used in echocontrast agents[8] such as Echogen™. Since the boiling temperature for this material is approximately 28–30 °C at 1 atmosphere pressure, individual droplets will be superheated at body temperature (37 °C). If a nucleation mechanism allows some droplets to boil and hence become bubbles, the low solubility of DDFP will allow the bubbles to persist in the circulatory system and provide sustained ultrasonic contrast.

[a)]Corresponding author.

2. Theory

The objective is to determine a bubble's size given knowledge of its acoustic backscatter strength at a single frequency. Inversion of the measurement requires a forward model that predicts the backscattered pressure field as a monotonic function of scatterer radius and nominal properties. We consider monochromatic plane waves incident upon an inviscid fluid/elastic sphere of radius a suspended in a fluid host, where both the sphere and the host materials are compressible and nonconducting, and the boundary conditions are the continuity of normal velocity and normal stress across the surface of the sphere. In this case, the far-field scattered pressure amplitude $p_s(r)$ can be expressed in the following form:[9]

$$p_s(r) = \left[\frac{P_0}{r} \exp(ikr) \right] \Phi, \tag{1}$$

where r is the distance from the center of the scatterer to the field point, P_0 is the amplitude of the incident plane wave, k is the wave number in the host fluid, and Φ is the angular distribution function that modulates an outgoing spherical wave given by

$$\Phi = \frac{i}{k} \sum_{m=0}^{\infty} (2m+1) \sin \eta_m \exp(-i\eta_m) P_m(\cos \theta). \tag{2}$$

In Eq. (2) P_m is the Legendre polynomial of order m and argument $\cos \theta$; θ is the scattering angle referenced to the forward direction ($\theta = 180°$ for backscattering), and η_m is the phase angle of the mth partial wave. The phase angle results from the imposition of the boundary conditions. The function Φ contains all the information regarding the size, dynamic response, and acoustic contrast of the scatterer. In the particular case of a fluid sphere, it can be expressed as follows:

$$\Phi = \frac{1}{k} \sum_{m=0}^{\infty} \frac{(2m+1)}{1+iC_m} P_m(\cos \theta) \tag{3}$$

where

$$C_m = -\cot \eta_m = \frac{-\dfrac{dy_m(x)}{dx} + \dfrac{y_m(x)}{j_m(x')} \dfrac{dj_m(x')}{dx'} \dfrac{\rho c}{\rho' c'}}{-\dfrac{dj_m(x)}{dx} + \dfrac{j_m(x)}{j_m(x')} \dfrac{dj_m(x')}{dx'} \dfrac{\rho c}{\rho' c'}}, \quad x=ka, \ x'=k'a, \tag{4}$$

where ρ and c are the density of and sound speed in the host fluid, respectively, and $j_m(x)$ and $y_m(x)$ are spherical Bessel functions of the first and second kind, respectively. A prime denotes the parameters of the fluid sphere. In this work, modes up to $m=10$ are summed.

The dynamics of DDFP bubbles less than 1 μm in radius, and hence acoustic response, should be dominated by the viscosity of the host fluid, μ. As previously shown,[10,11] viscosity shifts the resonance frequency of the backscattered signal to a higher value and even eliminates completely the resonance peaks in the backscatter versus frequency curves for sufficiently small bubbles. The following assumptions are made to include host fluid viscosity in the angular distribution function. First, viscosity is taken into account only in the monopole mode ($m=0$). Because the bubble's size is much less than the wavelength in the host fluid ($ka=0.0126$ for DDFP bubbles of radius 100 nm in water at 30 MHz), the monopole mode is the greatest contribution to the scattering strength. The Keller–Miksis equation[12] is used to describe these oscillations. Second, thermal damping is disregarded because it is two orders of magnitude less than viscous damping.[11] Third, the monopole term of the scattered pressure field is linear with respect to bubble radius perturbation. This assumption is valid because the acoustic pressure amplitude is much less than the atmospheric pressure in this work (negligible nonlinear distortion of re-

flected waveform). Linearization of the equation for far-field scattered pressure [Eq. (11) in Khismatullin[10]] leads, at $ka \ll 1$, to the following viscous correction added to the coefficient C_0:

$$i \frac{4\mu}{\rho cax^2}. \tag{5}$$

Thus, the forward-scattering model consists of gaseous DDFP suspended in water. The density and sound speed for the DDFP gas are taken to be 11.4 kg/m^3 and 93 m/s, respectively, and the host fluid is assumed to be pure water with density 993 kg/m^3, sound speed 1520 m/s, and viscosity 1 cP$=$0.001 Pa·s at 37 °C.

3. Apparatus and methods

Individual bubbles were convected through the focus of a 30-MHz acoustic transducer, driven in pulse–echo mode, using an apparatus based on that of Roy and Apfel (1990).[13] The acoustic beam axis was oriented horizontally and the trajectory of the flow was in the focal plane of the transducer and perpendicular to the beam axis. A 3.2-mm-diameter brass ball was used as a scattering target for alignment of the ultrasound beam in an acrylic tank filled with clean distilled water at 37 °C. Two measuring microscopes positioned in the horizontal plane (perpendicular and parallel, respectively, to the acoustic axis) were used to record the position of the focus. Later, a coaxial jet flow consisting of an outer sheath flow and inner plug flow was positioned to pass vertically through the acoustic focus, based upon the microscope position (the jet was visualized by seeding the inner flow with India ink and proper alignment was confirmed by observing increased backscatter from the jet when ink was present). The outer sheath flow consisted of distilled water from a gravity feed at a continuous rate of 225 ml/h, while the inner plug flow was degassed Ringer's solution driven by a syringe pump at a constant flow rate of 1.4 ml/h. The inner flow was introduced coaxially into the outer flow via a 30-gauge needle located upstream of a narrowing in a glass capillary tube. This tube's inner diameter at the jet outlet was approximately 200 μm, with inner flow diameter approximately 10 μm. The inner flow moved at nearly constant velocity (plug flow) vertically downward and into a suction drain (siphon) located approximately 1 cm below the acoustic focus.

A 0.2-μm Nalgene filter was used at the syringe outlet to minimize particulate contamination of the inner flow. India ink, polystyrene spheres in suspension, or DDFP emulsion was infused at a known rate from a computer-controlled syringe pump to help visualize the inner plug flow (ink), provide calibrated scatterers (polystyrene spheres), or supply unknown scatterers (DDFP emulsion). Employing separate ports for each of these "seed" flows into the inner flow helped avoid cross contamination.

The unbacked, 6.35-mm-diameter lithium niobate transducer was driven in pulse–echo mode with a 2-μs-duration, 30-MHz tone burst of 40 V peak-to-peak amplitude at a pulse repetition frequency (PRF) of 4 kHz. Transducer focal length was 25.4 mm, and 6-dB focal width was 270 μm. Gating and filtering electronics allowed the returned echoes to be displayed on a Tektronix 2455B analog oscilloscope.[13] A monitor output of the oscilloscope yields an exact duplicate of the displayed signal, scaled in amplitude so that a full-scale signal on the screen (10 divisions) corresponds to 1 V at the monitor output. This voltage was input into a Panametrics model 5607 gated peak detector (GPD). The dc output of the GPD was recorded synchronously by a computer using a 12-bit analog-to-digital converter card (NB-MIO-16X; National Instruments).

4. Calibration, data processing, and inversion

Upon establishing a stable coaxial jet flow, calibration data were obtained by infusing polystyrene spheres (3.02-μm mean radius; Duke Scientific Company) in the inner plug flow via an injection port. Scattering events were recorded for 60 s. Movie Mm. 1 shows a segment of raw data from the output of the GPD for the 6-μm-diameter polystyrene spheres. Each circle represents the amplitude of an ultrasonic pulse reflected from a polystyrene sphere as the scatterer was convected through the focus. The data take on the form of discrete peaks for, at a

PRF of 4 kHz, a target is interrogated about 9 times as it traverses the focus; the peak echo voltage generated by the passage of a given sphere determines the scattering strength for that sphere. However, at high concentrations, there is a risk of having more than one sphere in the focus at the same time. A peak-finding routine was used to identify each 9-point peak; such points are represented in Mm. 1 by red plus signs. This procedure served to reject multiple peaks associated with the near-simultaneous passage of multiple scatterers ("coincidence scattering") and also to reject small peaks resulting from noise. Since the jet velocity and PRF were nearly constant (independent of particle size), the peak width represents the transit time through the acoustic focus of an individual particle.

Mm. 1. Segment of output of gated peak detector (V) for 6-μm-diameter polystyrene spheres. Horizontal axis is time or pulse number at a PRF of 4 kHz. Circles represent instantaneous peak detector values; red plus signs denote peaks found that have four points of consistent slope on either side of the maximum.

The next step in the processing scheme was to estimate the maximum echo voltage for a given peak in the data stream, given that the particle is sampled about 9 times as it traverses the main lobe of the ultrasound beam, which we approximate as Gaussian for convenience. For each such candidate peak, a two-parameter nonlinear least-squares fit of the Gaussian function $y = A \exp(-t^2/\sigma)$ was made to the 9 points defining the peak. Variations in the amplitude parameter A and the width parameter σ for successive peaks arise from variations in particle size and liquid jet trajectory through the acoustic focus, respectively. From the mean radius supplied by the manufacturer, the system sensitivity parameters Φ and P_0 [Eq. (1)] may be calculated for elastic scattering (polystyrene spheres).

For each DDFP bubble, the width parameter σ provides an estimate of transit time through the acoustic focus, and can be used to discard noncompact scatterers such as DDFP bubble "pearl chains," or other coincidence scattering events. For DDFP backscattered data, all candidate peaks were discarded whose width parameters σ were larger than twice the standard deviation in σ for the polystyrene sphere data. Although there still may be some coincidence scattering present in the remaining data, the result is a potential overestimation of the bubble size, based upon the larger scattering cross section of multiple bubbles present in the acoustic focus as opposed to that of a single bubble. Thus, the remaining peaks were assumed to be individual microbubbles of DDFP, and their amplitude parameters A were used with viscous linear scattering theory to determine a conservative estimate of their individual radii. *Liquid droplets of DDFP would have to be larger than 15-μm radius to produce the observed backscatter, while the volume-weighted mean radius of DDFP droplets in the emulsion tested is only 50 nm.*

The DDFP emulsion was infused into the inner plug flow at a rate of 1 μl/h at 37 °C, resulting in an approximately 1000-to-1 dilution of the emulsion into the inner plug flow. When the pump was inactivated, the backscatter quickly returned to a constant level below 0.2 divisions.

5. Results

The center panel of Fig. 1 shows the radii inferred from the amplitude parameter A for each of 400 6-μm-diameter polystyrene spheres that have passed through the acoustic focus. The uppermost panel of Fig. 1 shows a linear elastic scattering theory curve, on which are plotted the radii of individual spheres as the result of inversion using the nominal properties for polystyrene:[13] 1110-m/s shear wave speed (elastic scatterer), 2380-m/s compressional wave speed, 1049-kg/m^3 density at 37 °C. In the lowest panel of Fig. 1, the distribution of polystyrene sphere sizes is centered at radius 3 μm and serves as the calibration data with reference to which the DDFP data are compared.

Movie Mm. 2 shows the raw data stream of backscatter echo amplitudes from diluted DDFP emulsion as it passed through the acoustic focus. Candidate peaks are marked with a red plus sign. All peaks with width parameters σ larger than 2 standard deviations of the width parameters for the polystyrene spheres were rejected as caused by noncompact scatterers.
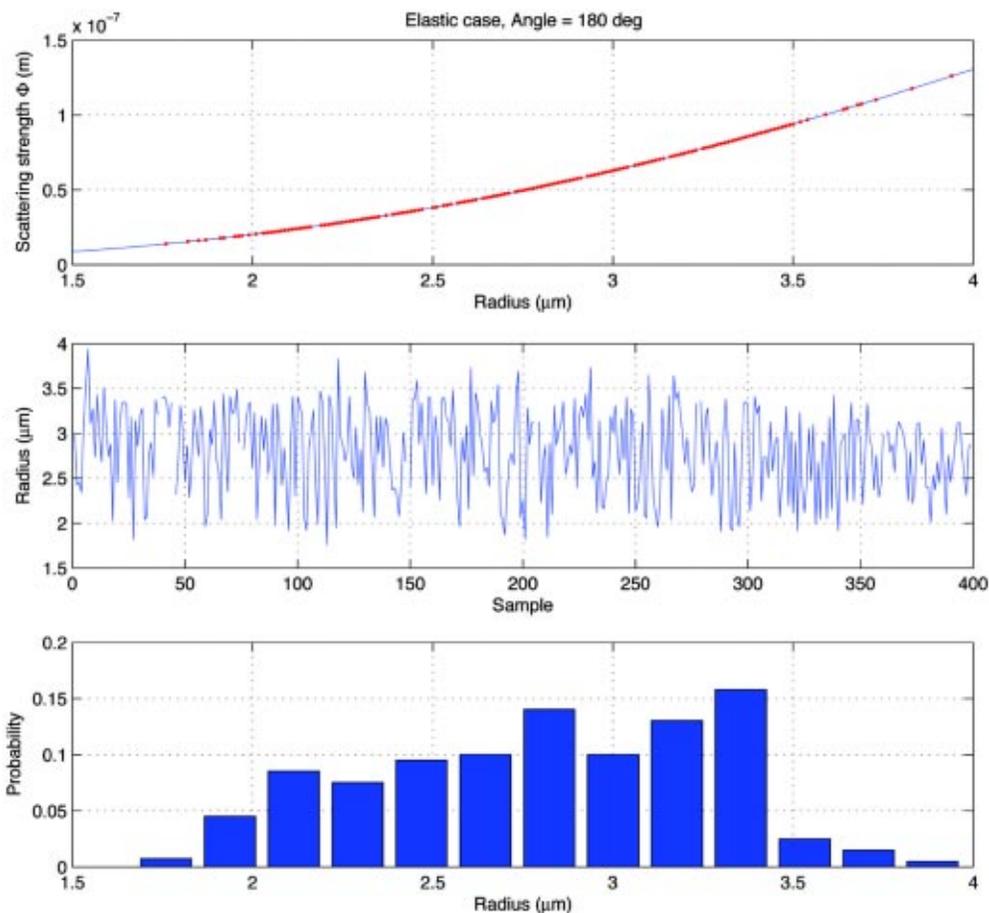
Fig. 1. Output of scattering inversion for 6-μm-diameter polystyrene spheres. Uppermost plot shows scattering cross-section curve and where these data fall upon it; middle plot shows inferred radius based upon inversion; lower plot shows probability histogram of microsphere radius, with mean value 3.02 μm as per manufacturer.

Remaining peaks, presumably single DDFP bubbles, are marked with an asterisk above the peak.

Mm. 2. Segment of output voltage of peak detector as a function of echo number for the DDFP emulsion at 37 °C. Note that, in comparison to Mm. 1, some peaks are broader, while others are the same width as those obtained from 6-μm-diameter polystyrene spheres. Since the jet flow rate was the same as for the polystyrene spheres, broader peaks indicate scatterers that are not compact with respect to the width of the acoustic focus (270 μm). Compact scatterer peaks are marked above with an asterisk.

The center panel of Fig. 2 shows the individual bubble radii inferred from the amplitude parameters of the remaining 2295 DDFP bubbles passing through the acoustic focus. The uppermost panel of Fig. 2 shows viscous linear scattering theory for DDFP bubbles below the critical radius, with monopole bubble resonance (shown in black) suppressed due to host fluid viscosity. The lowermost panel shows the result of inversion of the scattering data using the system sensitivity parameters obtained from the polystyrene spheres, as well as nominal parameters of DDFP gas. Thus, the mean DDFP microbubble radius is calculated to be about 130 nm with a standard deviation of about 50 nm. Sensitivity analysis shows that percentage variations in nominal properties produce changes in inferred radius of the same order.
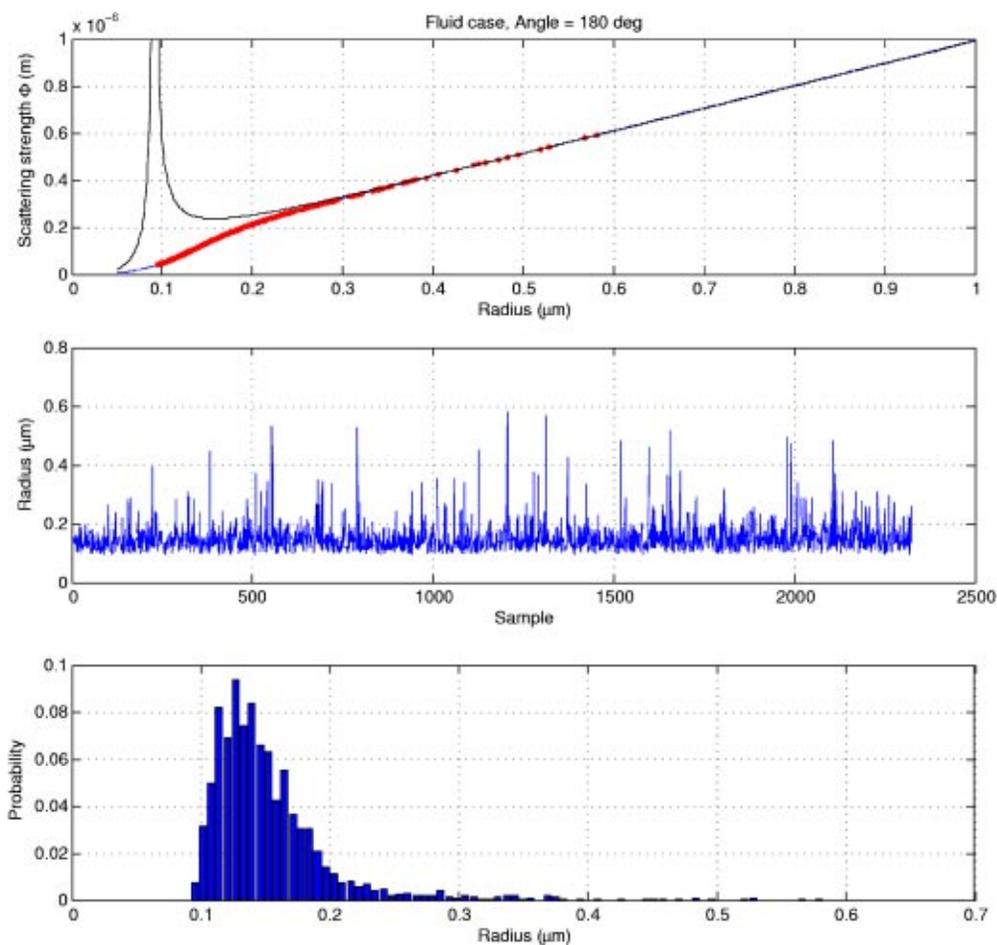
Fig. 2. Result of inversion using the compact scatterer data (asterisked) of Mm. 2 and the properties of polystyrene spheres (Fig. 1) for DDFP emulsion at 37 °C. Uppermost scattering theory curve (blue) shows suppression of resonance peak (black) due to viscosity of surrounding fluid for bubbles smaller than the critical radius. Mean bubble radius is 0.130 μm.

6. Summary and conclusions

The method presented here allows size determination of individual bubble radii smaller than other methods would permit. The DDFP microbubbles measured in this study were sufficiently small that viscosity of the surrounding fluid dominates their dynamics, leading to the removal of the resonance peak that inviscid theory would predict. Without a dominant resonance peak, inversion of the scattering data could be accomplished, allowing calculation of a size distribution for the DDFP bubbles between 100- and 200-nm radius, with diminishing numbers up to 600 nm. The size distribution is a conservative estimate (upper bound) since coincidence scattering (multiple bubbles in the focal region simultaneously) may have sometimes occurred.

Acknowledgments

References and links

[1] K.W. Commander and A. Prosperetti, "Linear pressure waves in bubbly liquids: Comparison between theory and experiment," J. Acoust. Soc. Am. **85**, 732–746 (1989).

[2] H.J. Bleeker, K.K. Shung, and J.L. Barnhart, "Ultrasonic characterization of Albunex®," J. Acoust. Soc. Am. **87**, 1792–1797 (1990).

[3] M. Nicholas, R.A. Roy, L.A. Crum, H. Oguz, and A. Prosperetti, "Sound emissions by a laboratory bubble cloud," J. Acoust. Soc. Am. **95**(6), 3171–3182 (1994).

[4] G. Kapodistrias and P.H. Dahl, "Laboratory studies on scattering from bubbles located close to an air-water interface," J. Acoust. Soc. Am. **111**(5), 2345 (2002).

[5] W.P. Arnott and P.L. Marston, "Optical glory of small freely rising gas bubbles in water: observed and computed cross-polarized backscattering patterns," J. Opt. Soc. Am. A **5**(4), 496 (1988).

[6] W.T. Shi, F. Forsberg, J.S. Raichlen, L. Needleman, and B.B. Goldberg, "Pressure dependence of subharmonic signals from contrast microbubbles," Ultrasound Med. Biol. **25**(2), 275–283 (1999).

[7] T.R. Porter, F. Xie, S. Li, A. D'Sa, and P. Rafter, "Increased ultrasound contrast and decreased microbubble destruction rates with triggered ultrasound imaging," J. Am. Soc. Echocardiogr **9**(5), 599–605 (1996).

[8] J.M. Correas and S.D. Quay, "Echogen emulsion: a new ultrasound contrast agent based on phase shift colloids," Clin. Radiol. **51**, 1–11 (1996).

[9] A.E. Hay and R.W. Burling, "On sound scattering and attenuation in suspensions," J. Acoust. Soc. Am. **72**(3), 950–959 (1982).

[10] D.B. Khismatullin, "Resonance frequency of microbubbles: Effect of viscosity," J. Acoust. Soc. Am. **116**, 1463–1473 (2004).

[11] D.B. Khismatullin and A. Nadim, "Radial oscillations of encapsulated microbubbles in viscoelastic liquids," Phys. Fluids **14**, 3534–3557 (2002).

[12] J.B. Keller and M. Miksis, "Bubble oscillations of large amplitude," J. Acoust. Soc. Am. **68**, 628–633 (1980).

[13] R.A. Roy and R.E. Apfel, "Mechanical characterization of microparticles by scattered ultrasound," J. Acoust. Soc. Am. **87**, 2332–2341 (1990).